Spectral and dynamical hints on the time scale of preparation of the 5 April 2003 explosion at Stromboli volcano

Roberto Carniel, Ramon Ortiz, and Mauro Di Cecca

Abstract: Stromboli volcano is well known for its continuous strombolian activity. Moreover, the volcano occasionally shows effusive phases, the latest in 1985–1986. On 28 December 2002 Stromboli entered a new effusive phase, accompanied by different paroxysmal events that led to considerable hazards for inhabitants and tourists on the island of Stromboli. On 30 December 2002 a major sector collapse affected the Sciara del Fuoco slope and initiated a tsunami. On 5 April 2003 a powerful explosion, which can be compared in size with the most recent explosion in 1930, covered a large part of the normally tourist accessible summit area with bombs. As this explosion was not forecasted, although the island was by then effectively monitored by a dense deployment of instruments, in this paper, we tackle the problem of highlighting the time scale of preparation of this event and conduct a search for possible precursors. For this purpose, we analyze the seismic data preceding the paroxysm with spectral and dynamical methods, highlighting that this paroxysmal event can be seen as the final result of a dynamical phase that started at least 2.5 h before the event. Therefore, this is the time scale during which the search can and should be made for possible precursors. Moreover, the application of the "material failure forecast" method suggests that this final dynamical phase may be just the final acceleration of a process that was building up for at least several days prior to the event.

Résumé : Le Stromboli est bien connu pour son activité strombolienne continue. De plus, le volcan montre parfois des phases effusives, la dernière remontant à 1985–1986. Le 28 décembre 2002, le Stromboli est entré dans une nouvelle phase effusive, accompagnée de différents événements de paroxysme qui ont constitué un danger considérable pour les habitants de Stromboli et les touristes. Le 30 décembre 2002, un grand secteur s'est effondré, affectant la pente Sciara del Fuoco et causant un tsunami. Le 5 avril 2003, une explosion puissante, d'une grande violence, comparable à celle de 1930, a recouvert de bombes volcaniques une bonne part du sommet normalement accessible aux touristes. Comme cette explosion n'était pas prévue, bien que l'île fut à ce moment fortement instrumentée, nous discuterons dans cet article du problème de souligner l'échelle de temps de la préparation menant à cet événement et nous chercherons des précurseurs possibles. À cette fin, nous analysons les données sismiques précédant le paroxysme par des méthodes spectrales et dynamiques, soulignant que ce paroxysme peut être perçu comme le résultat final d'une phase dynamique qui a débuté au moins environ 2,5 heures avant l'événement. Cela représente donc l'échelle de temps selon laquelle l'on pourrait et l'on devrait rechercher des précurseurs possibles. De plus, l'application de la méthode « Material Failure Forecast » suggère que cette phase dynamique finale soit seulement l'accélération finale d'un processus qui se préparait au moins au cours des derniers jours.

[Traduit par la Rédaction]

Introduction

Stromboli volcano, Italy, is the prototype for strombolian activity, observed since at least A.D. 3–7 (Rosi et al. 2000) thanks to an efficient conduit supply (Kazahaya et al. 1994; Stevenson and Blake 1998). The strombolian bursts can be produced by a gas slug (Wilson and Head 1981; Parfitt and Wilson 1995) that collapses at a physical boundary (Jaupart and Vergniolle 1989; Thomas et al. 1993; Ripepe et al. 2001). Occasionally, paroxysmal phases are observed (Barberi et al. 1993; Jaquet and Carniel 2003) and are a danger to the numerous tourists visiting the area; one was killed in 2001 (Alean et al. 2005; Barberi et al. 2001). Francalanci et al. (2004) showed that Stromboli erupts two sharply distinct magmas, one of which (low-porphyritic and volatile-rich magma) plays a major role in these paroxysmal events.

Received 14 February 2005. Accepted 15 September 2005. Published on the NRC Research Press Web site at http://cjes.nrc.ca on 27 February 2006.

Paper handled by Associate Editor J.D. Greenough.

R. Carniel[1] **and M. Di Cecca.** Dipartimento di Georisorse e Territorio, Università di Udine, Via Cotonificio 114, 33100 Udine, Italy.
R. Ortiz. Departamento de Volcanología, Museo Nacional de Ciencias Naturales, Consejo Superior de Investigaciones Cientificas (CSIC), Madrid, Spain.

[1]Corresponding author (e-mail: roberto.carniel@uniud.it).

 doi:10.1139/E05-093

With respect to time scales, Ripepe et al. (2002) identified two (degassing and explosive) regimes, linked to the fresh gas-rich magma supply rate, that alternate on a 5–40 min time scale. For longer time scales, Carniel and Di Cecca (1999) identified days- to weeks-long dynamical phases, sometimes separated by abrupt transitions, that can be associated with paroxysmal phases but not with tectonic regional earthquakes (Falsaperla and Spampinato 1999; Falsaperla et al. 2003), as shown, for example, at Ambrym volcano (Carniel et al. 2003). In terms of possible precursors, Carniel and Iacop (1996*b*) showed that paroxysmal phases are sometimes preceded by an increase in the lower frequency content in the tremor. Due to the complexity of the physical processes involved, a stochastic (Jaquet and Carniel 2001, 2003) or dynamical approach (Carniel and Di Cecca 1999; Carniel et al. 2003) is often a more appropriate choice for short- to medium-term forecasts aimed, for example, at scheduling tourist excursions when the volcanic hazard is lower.

On 28 December 2002, an effusive eruption (Alean et al. 2005) marked the most significant effusive episode since 1985–1986. On 30 December at 13:15 and 13:22, two landslides, totalling ~11×10^6 m^3, formed along the Sciara and reached the sea (Calvari and Stromboli On Line 2002; Bonaccorso et al. 2003), causing tsunami waves that damaged the villages of Stromboli and Ginostra. The implications of similar, but larger scale events, which happened at least four times in the last 13 000 years, have recently been investigated by Tibaldi (2004). The effusive eruption induced other considerable morphological changes before it ended on 21–22 July 2003 (Calvari 2003b) and showed the most energetic event at 0712 GMT on 5 April 2003. The event started with a reddish ash emission related to collapses within the craters and was soon replaced by emissions of darker juvenile material from the northeast crater and then similar emissions from the southwest crater (see Fig. 1), with the appearance of a dark, mushroom-shaped cloud rising about 1 km above the summit (Calvari 2003b). Bombs, ash, and blocks affected most the of the western sector and the village of Ginostra; the volcano top above 700 m above mean sea level (amsl) was completely covered by bombs, including metre-sized bombs (Alean et al. 2005), and scientific equipment, including the seismic station of the University of Udine, was damaged or destroyed (see later in the paper). In this paper, we tackle the problem of highlighting the time scale of preparation of this event and conduct a search for possible precursors. The strombolian events are superimposed on a volcanic tremor strongly related to variations in the fluid–conduit pressure field (Martinelli 1997) and the subject of contradictory interpretations (see, e.g., Ripepe and Gordeev 1999; Urquizú and Correig 1999, and the references therein), correlations with other geophysical parameters (Ripepe et al. 2002), and statistical analyses (Falsaperla et al. 1998). A recent review (Konstantinou and Schlindwein 2002) has highlighted that, although probably generated by different processes at different locations (Stromboli (Carniel and Di Cecca 1999; Urquizù and Correig 1999), Kilauea (Chouet and Shaw 1991), Ambrym (Carniel et al. 2003), Soufrière Hills (Correig and colleagues)[2]) or simply at different times, volcanic tremors share the properties of nonlinearity, nonstationarity, and stochasticity. Nonstationarity is a key characteristic, as it offers the possibility of monitoring changes in parameters derived from an experimental time series and their possible use in forecasting (Carniel and Di Cecca 1999) or at least highlighting different regimes (Ripepe et al. 2002; Carniel et al. 2003; Harris et al. 2005; Jones et al. 2005). In the stochastic approach (Jaquet and Carniel 2001, 2003), the systematic monitoring of the evolution of the stochastic parameters computed via geostatistical models over different time windows was introduced recently (Jaquet et al. 2005). Moreover, chaotic deterministic systems can mimic stochastic models, and from a phenomenological modelling point of view (Correig and colleagues)[2], it is not necessary for the monitoring model to reflect the physical laws behind the process as long as dynamical transitions can still be identified. This is similar to the application of linear spectral analysis to a nonlinear system, which is carried out because it is an efficient approximation that can be used for monitoring, notwithstanding the fact that frequencies do not really satisfy the hypothesis of the superposition of the effects. It is obvious, however, that a nonlinear method is still the best way to analyse nonlinear time series, and this is what we do in the following.

Data and methods

Few seismic stations have operated continuously on the island of Stromboli. One of the longest time series available comes from an automatic seismic station installed in 1989 by the Dipartimento di Georisorse e Territorio of the University of Udine (Beinat et al. 1994) with the purpose of studying the long-term evolution of strombolian activity (Carniel and Iacop 1996*a*). The summit station, based on three Willmore MKIII/A seismometers (eigenfrequency $f_0 = 0.5$ Hz), is located at 800 m asl and about 300 m from the craters (Beinat et al. 1994). During this last effusive phase, the hardware and software of the receiving station were upgraded by the Consejo Superior de Investigaciones Cientificas (CSIC) for continuous acquisition and internet data transmission. Data are now sampled with 16 bits (96 dB) at 50 Hz (Ortiz et al. 2001).

Although a dense network of monitoring equipment installed by the Italian Civil Defence was operating at the time of the 5 April 2003 paroxysmal event, the explosion was not forecasted by any evident change in the data. In the following, we examine in detail the dynamics of the seismic data recorded by our station before this paroxysmal event (Fig. 1) with the first purpose of understanding the time scale during which the paroxysm built up. This has two main objectives: the first is to furnish a time scale during which the search should be made for precursors of similar events, and the second is to furnish a time scale that could be used to model the phenomenon that led to this paroxysm.

We first examine the time (n) evolution of the seismic intensity prior to the paroxysmal event. We subdivide the raw data in windows of 120 s (i.e., $N = 6000$ sample points at 50 Hz), with a 50% overlap so that two successive windows are separated by 1 min, and we compute the real-time seismic amplitude measurement (RSAM) intensity as defined by Endo and Murray (1991) after having removed the instru-

[2] Correig, A.M., Urquizù, M., Carniel, R., and Vila, J. In preparation. A phenomenological model for volcanic tremors.

Fig. 1. (*a*) Raw seismic data (vertical component) showing the paroxysmal event, as acquired by our summital seismic station. (*b*) Photograph (courtesy of Sergio Ballarò) showing the paroxysmal event close to its climax.

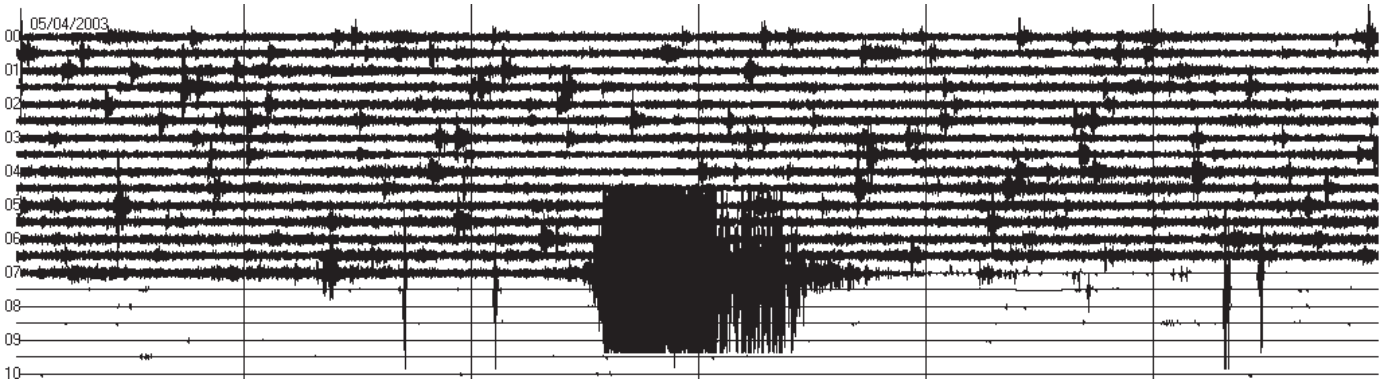

(a)

(b)

mental offset to obtain the instant amplitude S_i to be average over the window length N.

$$\text{RSAM}\,(n) = \frac{1}{N}\sum_{i=n}^{n+N} S_i$$

We proceed with the analysis of the evolution of the spectral content of the seismic signals in the three components over the same time windows. After removal of the offset, a fast Fourier transform (FFT) is applied with a 10% Hanning window. The amplitude is then normalized to the range [0, 1] to highlight relative spectral changes independently of amplitude variations, which were investigated previously. The most energetic part of the spectrum (0.5–10.5 Hz) is divided into 40 bins, 0.25 Hz wide, and integrated values are normalized to a unitary sum to obtain the relative distribution of the energy only across this frequency range. Scalar parameters are also derived from the spectrogram. In

particular, the dominant frequency is defined for each time window as the bin where the maximum spectral value is observed, and average frequency is defined as the average of the bins center frequencies, each weighted by its own spectral value (Carniel and Di Cecca 1999), to represent the center of mass of the spectral distribution.

As for the dynamical analysis, we perform the embedding of the data contained in each time window, following the time delay method (Packard et al. 1980), i.e., seeing each experimental time series as an observable derived from the state variables $X(t_n)$ of a dynamical system that evolves with time t_n.

$$X(t_{n+1}) = F[X(t_n)]$$

Two parameters are needed to perform this embedding, i.e., reconstructing a multidimensional (pseudo) state space from the single time series of choice. The first parameter, called delay time, is the time that separates each pair of coordinates. The second parameter is the number of coordinates we have to use for the reconstruction, called embedding dimension (Carniel and Di Cecca 1999; Carniel et al. 2003).

The choice of the delay time should maximize the independence between the coordinates used in the reconstruction. For this reason, methods typically used to choose the delay time involve finding the first zero of the autocorrelation function or the first minimum of the redundancy, also known as mutual information. On the contrary, the optimal embedding dimension is the one for which all the dynamics, i.e., the trajectories of the attractor underlying the volcanic dynamical system, are fully unfolded. One of the most commonly used methods to choose the dimension, known as the false nearest neighbours (FNNs) method (Kennel et al. 1992), is of pure geometrical character. The dynamics are completely unfolded when, moving from one dimension (i) to the next dimension ($i + 1$), there is no more separation of false neighbouring points, i.e., points that only appear to be near because of the projection onto a space that is too low dimensional. The percentage of remaining FNNs is a measure of the percentage of the dynamics that cannot be explained in a given dimension. Being noise infinite-dimensional, we can never reach a zero percentage when we are dealing with experimental, noisy time series.

Singular value decomposition (SVD) is a completely independent method to assess the dimensionality of the dynamical system generating an experimental time series. As a first step, the original scalar time series $\{x_i\}_{i\,=\,1\ldots n}$ is used to build a trajectory matrix

$$\mathbf{X} = \begin{Bmatrix} w_1(m) \\ w_2(m) \\ w_3(m) \\ \vdots \\ w_{n-m+1}(m) \end{Bmatrix} = \begin{Bmatrix} x_1 & x_2 & \cdots & x_m \\ x_2 & x_3 & \cdots & x_{m+1} \\ x_3 & x_4 & \cdots & x_{m+2} \\ \vdots & \vdots & & \vdots \\ x_{n-m+1} & x_{n-m+2} & \cdots & x_n \end{Bmatrix}$$

which is by definition a Hankel matrix of the original time series, being $X_{i,j} = x_{i+j-1}$. Each row of the matrix $w_i(m)$ is called an m window or an embedding window. It is worthwhile to note that all the scalar values are used here, i.e., an implicit time delay equal to the sampling period is assumed for the embedding. To compensate for this, the length m of each embedding window should be generally higher than before to capture the whole behaviour of the system. Several criteria can be used to suggest the value of the embedding window duration, $\tau_w = m\tau_s$, where τ_s is the sampling period. Broomhead and King (1986) suggest that $(2f + 1)\tau_s$ is a lower bound, where f is the dimension of the attractor (which is not known) and $\tau^* = 2\pi/\omega^*$ is an upper bound, where ω^* is the band-limiting frequency. In our case, we chose an embedding dimension of $m = 20$. The idea is now to project the matrix $\mathbf{X}$ over an m-dimensional space. This is done by computing the covariance matrices and determining a spectral decomposition

$$\mathrm{X}\mathrm{X}^{\mathrm{T}} = \Phi_1 \Lambda_1 \Phi_1^{\mathrm{T}}$$

where Φ_1 is a real orthonormal matrix, and Λ_1 is a real diagonal matrix. By ordering the matrix Λ_1 so that the diagonal values σ_i^2 are in decreasing order, we obtain the possibility of determining an optimal base in the sense described previously, i.e., a base where each vector has a lower importance than the previous one in the construction of the signal. Such importance is given by the weight σ_i of each singular value of the matrix $\mathbf{X}$. In this way, we can finally weight the importance of a given (low) number k of first dimensions and monitor accordingly how this suitably defined, low-dimensional, dynamical subsystem gains or loses importance with respect to the remaining (m–k) dimensional space. In summary, this can allow us to better characterize numerically the fact that the system "evolves towards a simpler one." In summary, we define the following ratio and monitor its time evolution.

$$r_k = \sum_{j=1}^{k} \sigma_j \,/\, \sum_{j=k+1}^{m} \sigma_j$$

Lastly, in the hypothesis that an anomalous phase is identified by one or more of the methods described, the following natural question arises: when should we expect the paroxysmal event to happen? To try to answer this question, we use the material failure forecast method (FFM). Voight (1988, 1989), Voight and Cornelius (1991), and Cornelius and Voight (1995) proposed this method for the Mount St. Helens eruption. Empirical observations of hyperbolic acceleration of the growth of a parameter can be traced back to Tokarev (1963), however. Recent examples of applications include the Colima (De la Cruz-Reyna and Reyes-Dávila 2001) and Villarrica (Ortiz et al. 2003) volcanoes. The main idea is to apply the differential equation modelling the material failure.

$$\frac{\mathrm{d}^2\Omega}{\mathrm{d}t^2} = A\left(\frac{\mathrm{d}\Omega}{\mathrm{d}t}\right)^{a}$$

where Ω is an observable (deformation, seismic energy, etc.), and A and α are two experimentally determined parameters. An experimental series, assumed to be the solution of such an equation, can be used to extrapolate the descending sections of the inverse of the observable to obtain a forecasted time of an eruption. We use as the observable the RSAM defined earlier, where the amplitude in the sum, following De la Cruz-Reyna and Reyes-Dávila (2001), is substituted by the energy, directly proportional to the rate at which strain is released by the ongoing seismic process.

Fig. 2. (*a*) Time evolution of seismic intensity (RSAM in arbitrary units or A.U.) computed over 50% overlapping, 120 s windows from the three single components. The time axis covers the first 5 days of April 2003 and goes from 1 April at 0000 GMT (hour 0) to 5 April at 0800 GMT (hour 104). A moving average of 5 min is applied for graphical smoothing. (*b*) Detail of the time evolution of the seismic intensity during the morning of 5 April 2003. Time axis hours as in (*a*), but no moving average was applied.

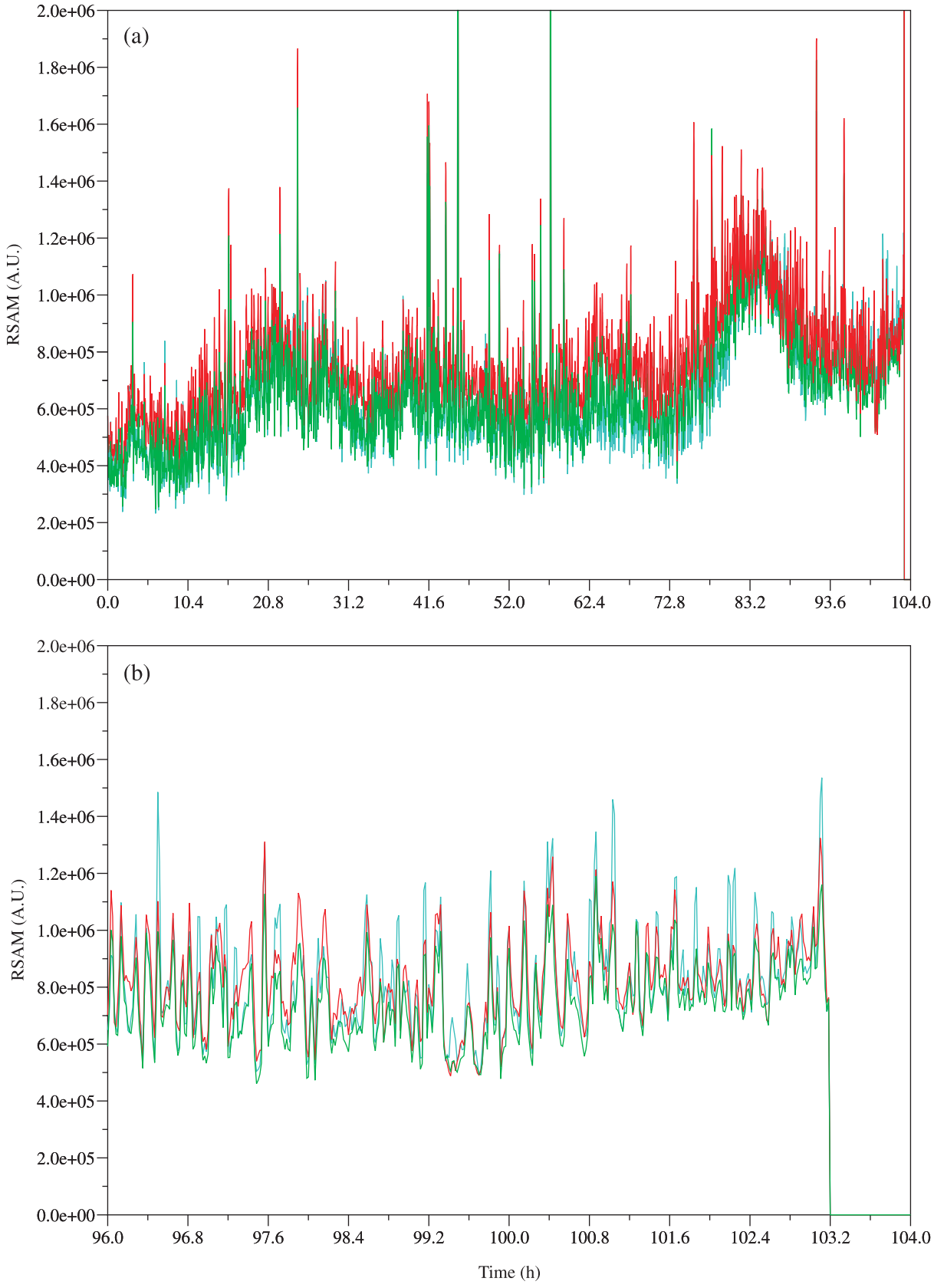

Fig. 3. Spectrogram of the first 5 days of April 2003 for the radial component. Each column represents a time window of 120 s with a 50% overlap. The vertical frequency axis is subdivided into 40 bins, each 0.25 Hz wide. Each time window is normalized so that the sum of the bin values is equal to 1. A moving average of 5 min is applied for graphical smoothing.

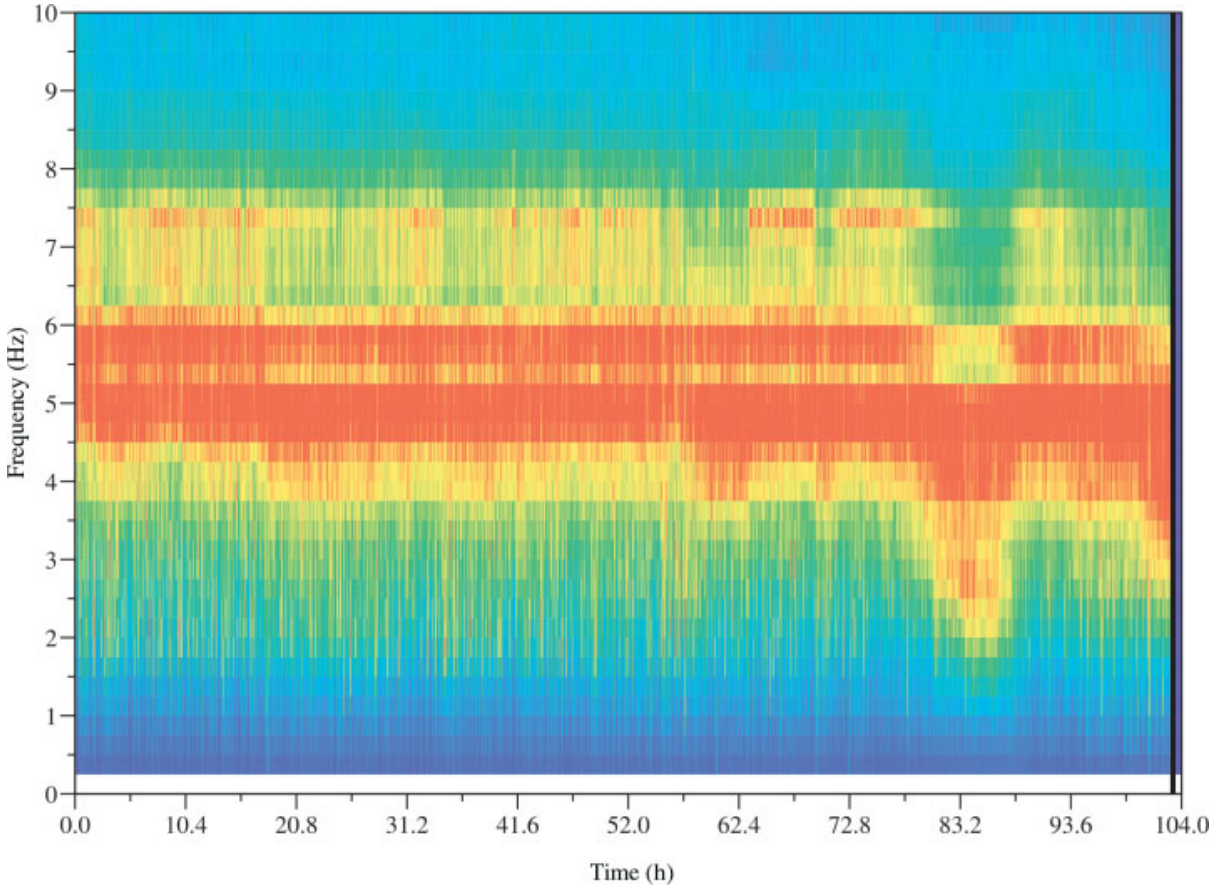

Results

The time behaviour of the RSAM is shown in Fig. 2*a* for the first 5 days of April. Particularly high or low values of this parameter are not evident during the 5 days prior to the paroxysmal event or during the few hours before the event when the evolution is examined in detail (Fig. 2*b*). This simple parameter, therefore, definitely cannot act as a precursor of the paroxysm. It is interesting to note in Fig. 2*b*, however, that the seismic intensity shows a consistently steady increase before the paroxysmal event. Although this increase is moderate, as the absolute values reached before the explosion are absolutely comparable to those assumed during the previous days, this period of consistent behaviour (2.5 h) can be the first hint of the time scale of preparation of the paroxysmal event.

The computed spectrogram is shown in Fig. 3 for the first 5 days of April. Again, no particularly anomalous variations can be seen in the frequency distribution which could be used as a precursor of the explosion, as even more pronounced phases, like that around hour 85 and as discussed in more detail later in the paper, are evident in the graph. Once again, we see a consistent trend during the 2.5 h before the paroxysmal event, however, during which the spectral energy slowly, but steadily, moves from the 4.5–6.0 Hz range to the 3.0–4.5 Hz range. The time evolution of the average frequency and the dominant frequency, not shown for brevity, again does not present strongly anomalous values before the paroxysm but does show a consistent behaviour in the last 2.5 h before the explosion, with the dominant frequencies seen in the different components getting closer to one another and the average frequencies showing a consistent, almost monotonically decreasing trend in all the components.

In Fig. 4*a*, we plot the time evolution of the first zero of the autocorrelation function for all 1 min time windows of the vertical component for the first 5 days of April. Once again, although the values assumed by the parameter are in the same range as those of the previous days, there is a consistent, 2.5 h long dynamical phase before the paroxysm, where the value for the delay time suggested by the autocorrelation function, which guarantees linear independence between any pair of successive coordinates, shows a clear decreasing trend.

The time evolution of the other estimator of the optimal delay time, i.e., the redundancy, which guarantees more generally that the information content we can infer from one coordinate to the other is minimum, is shown in Fig. 4*b*. In this case an even more clearly monotonous decreasing trend is shown in the 2.5 h before the paroxysmal event. In summary, both delay time estimators indicate a consistent dynamical phase before the explosion.

Once we have an estimate for the delay time, we can pro-

Fig. 4. (*a*) Time evolution of the first zero of the autocorrelation function for the vertical component during the first 5 days of April 2003. Each datum represents a time window of 120 s with a 50% overlap. (*b*) Time evolution of the first minimum of the mutual information for the vertical component during the same period. Each datum represents a time window of 120 s with a 50% overlap.

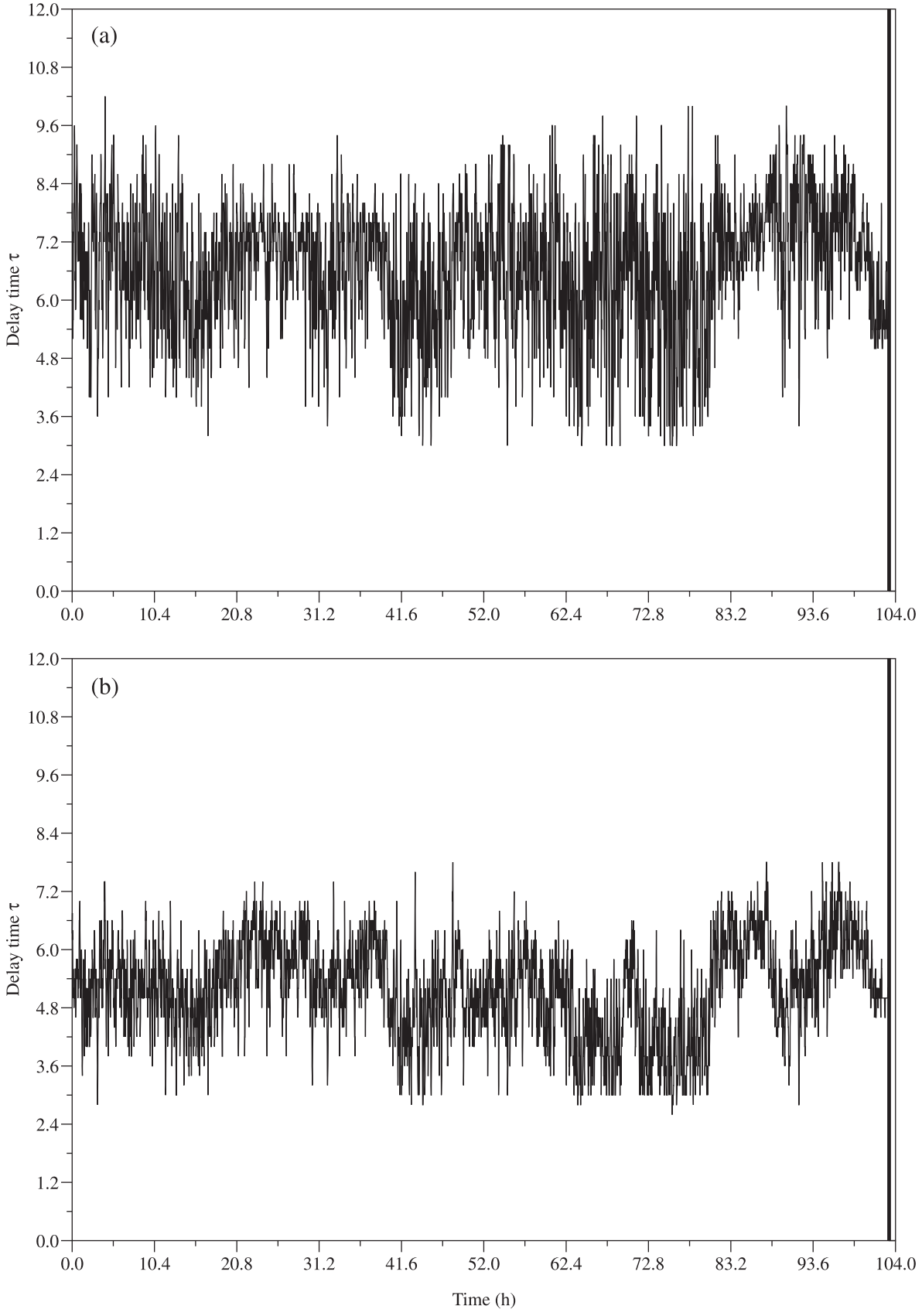

Fig. 5. Time evolution of the percentage of FNN in dimension 8 during the first 5 days of April 2003. Each datum represents a time window of 120 s with a 50% overlap. A moving average of 5 min is applied for graphical smoothing.

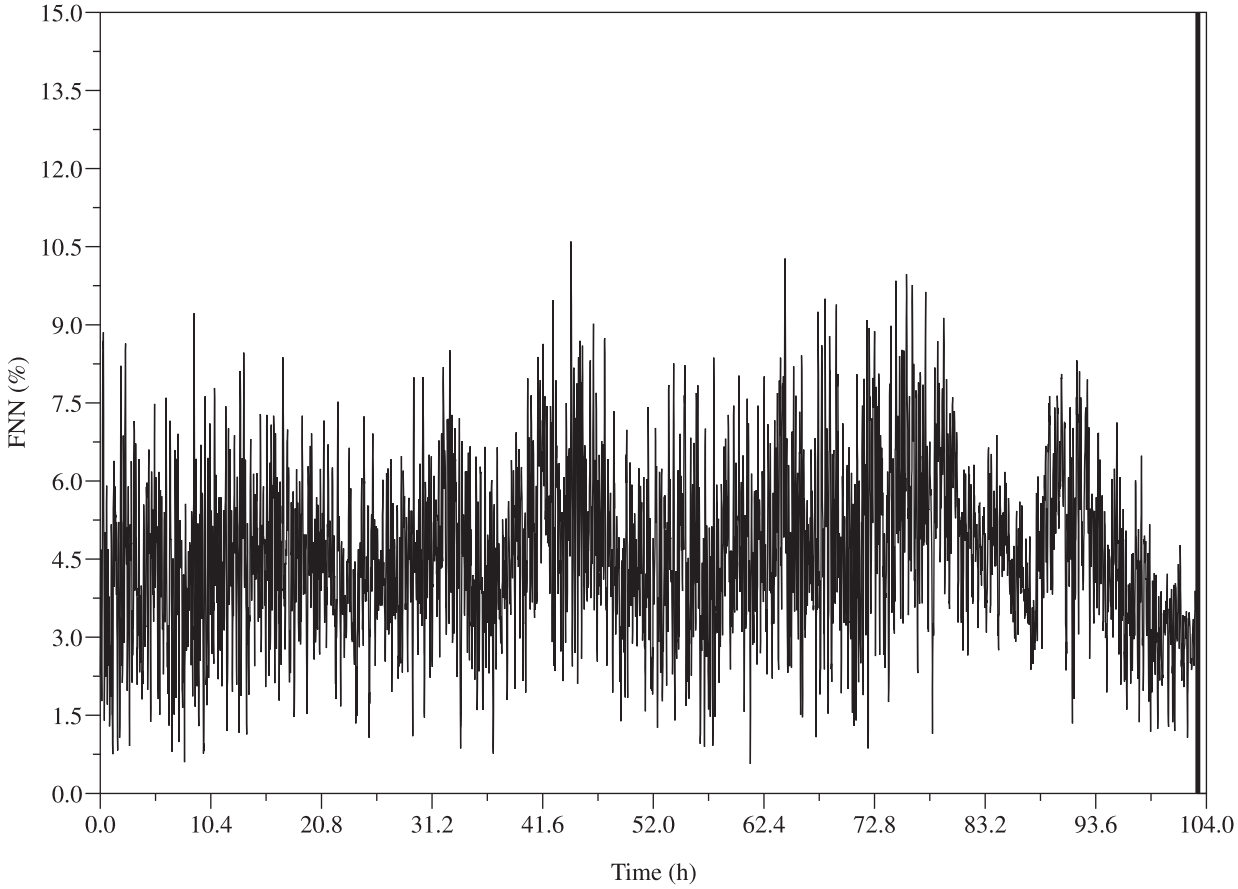

ceed with the computation of the percentages of FNNs, for all the time windows and for all the values of the dimension parameter, increasing it one by one from 1 to 9. In a given time window, such a percentage tends to decrease with an increase in the embedding dimension. As expected for a noisy series, however, it never goes to zero. In Fig. 5, we show the time evolution of the percentage of FNNs remaining in dimension 8. This, as outlined previously, is a proxy for the percentage of system dynamics that requires dimensions higher than 8 to be unfolded. Before the paroxysmal event, again a consistent trend is highlighted. The percentage of FNNs decreases steadily during the few hours preceding the event. In this case, the beginning of this phase is not as clear as that for the other parameters and may start slightly before.

It is worth noting that in this case the FNNs shown for dimension 8 reach their lowest values over the entire plotted period (covering the first days of April 2003) just before the paroxysmal event. It is also important to note that, as already shown by Carniel and Di Cecca (1999), these variations in the FNNs cannot be a simple consequence of a changing delay time, as this choice has a small influence on the computed FNN value. So, this parameter would not only tell us that there is a "special" dynamical phase before the paroxysm, but could also act as a possible precursor for the paroxysm itself. Performing further analyses and looking back at the time evolution of the FNNs in dimension 8 for the last days of March 2003, however, when no paroxysmal phase was observed (graph not shown for brevity), we discover other examples where such a low percentage of FNNs (below 3%) is reached. So, FNNs are not yet the precursor we are looking for.

It is still important, however, that before the paroxysmal event, we observe a steadily decreasing number of FNNs for a given dimension. This means that the system dynamics become better and better explained in that dimension, i.e., the dynamical process becomes simpler and simpler. We cannot go much farther than that, as the delayed coordinates method creates an embedding that is not optimal, as there is no concern regarding, for example, the evaluation of the importance of the different pseudo-state variables that are used as coordinates for the reconstruction. Not only do the different coordinates have no straightforward physical meaning, besides the fact that they are delayed values of the original velocity record, but also we cannot ever say, for example, that the fourth coordinate out of eight, whatever it means, is more important than the third or fifth in the construction of the signal.

A further step would be to weight each dimension by evaluating its contribution to the explanation of the global dynamics. In this way, not only could we say how good an embedding in dimension 8 is, but we would also be able to examine in detail the importance that each single dimension out of the total of 8 has in the construction of the signal. This requires the use of the SVD. In Fig. 6, we plot, for each

Fig. 6. Time evolution of the inverse of the singular value decomposition ratio r_k for $k = 4$ (see text for further details) during the first 5 days of April 2003. Each datum represents a time window of 120 s with a 50% overlap.

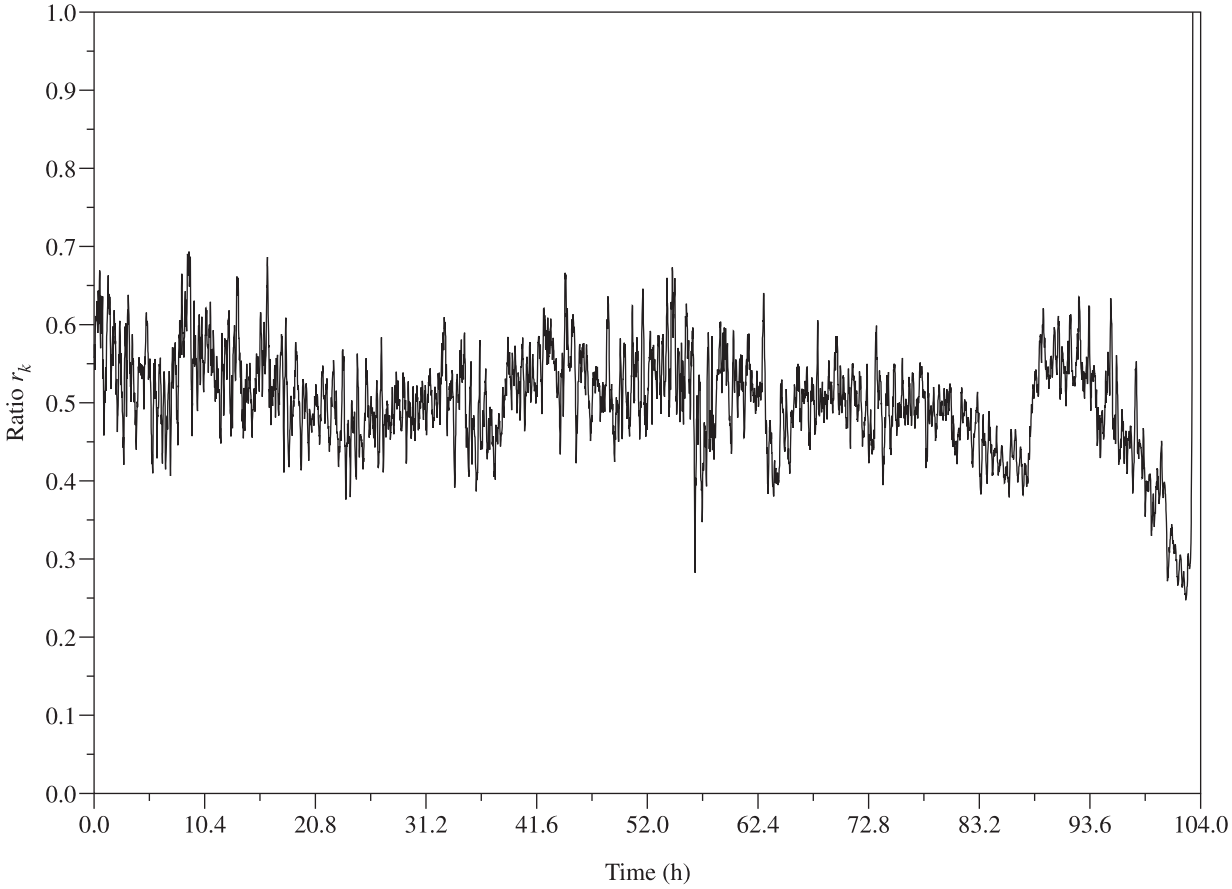

2 min window, the inverse of the ratio r_k for $k = 4$ as a function of time. The first result is that, as we could reasonably expect, the fact that before the paroxysmal phase the system becomes simpler and simpler is reflected by a steady decrease in the observable, which basically measures the need for the dimensions greater than $k = 4$ to explain the dynamics of our system. However, this time the ratio shows, just before the paroxysm, the lowest value recorded over the whole interval of analysis (first days of April). The fact that no similar behaviour can be observed (see Fig. 7) this time, looking back at the last days of March, places additional confidence in this parameter as a possible precursor of the paroxysm. Although we can say, however, that (*i*) we have identified an "anomalous" dynamical phase and (*ii*) the values shown for the parameter are so anomalous that they were never assumed in the previous two weeks, there is a major problem to be solved. When, even in the course of an anomalous phase like this one, should we expect an explosion to happen? To try to answer this question, we use the FFM.

Window length used for this purpose is 20 min, and we examine both the RSAM computed over the raw data (Fig. 8*a*) and that computed over a band-pass-filtered signal (finite impulse response (FIR), center frequency 1.2 Hz, attenuation –80 dB at 0.5 and 2.0 Hz) (Fig. 8*b*). The filter is designed from the spectrogram to optimize the stability of 1/RSAM on one side and its sensitivity to changing volcanic activity on the other.

A plot of the RSAM is shown in Fig. 8*a* as a reference, computed over time windows of 1 min. In Figs. 8*b* and 8*c* we simulated a series of forecasts to "simulate the future in the past." Several decreasing trends are observed in the plots, often preceding the major explosions indicated by the vertical arrows. We have to remember, however, that the paroxysm is significantly more energetic with respect to all the other explosions (see Fig. 1) and therefore is the main explosion we want to forecast. At a given time (4 April 2003 at 1230 GMT), we therefore performed a fitting of the inverse of the observable (1/RSAM) using the data from the previous 24 h (3 April 2003 at 1230 GMT to 4 April at 1230 GMT), where this parameter shows a decreasing trend. The extrapolation of the fitting line, more precisely the time of its intersection point with the horizontal axis, is the forecasted time of occurrence of the paroxysm. The fit of Fig. 8*b* is obtained applying the computation of the inverse of the RSAM over 20 min windows of raw, unfiltered data. Although there is a clear decreasing trend that can be fitted, the forecasted time of the paroxysm would be 6 April at 0100 GMT.

Things improve if we introduce the spectral content. Applying the band-pass filter described previously to the data before computing the RSAM and its inverse better highlights the decreasing trend, and consequently improves the relative fitting line, which now intersects the horizontal axis on 5 April at 1500 GMT, the expected time for the paroxysm according to the FFM.

Fig. 7. Time evolution of the inverse of the singular value decomposition ratio r_k for $k = 4$ (see text for further details) during the period 25–31 March 2003. Each datum represents a time window of 120 s with a 50% overlap.

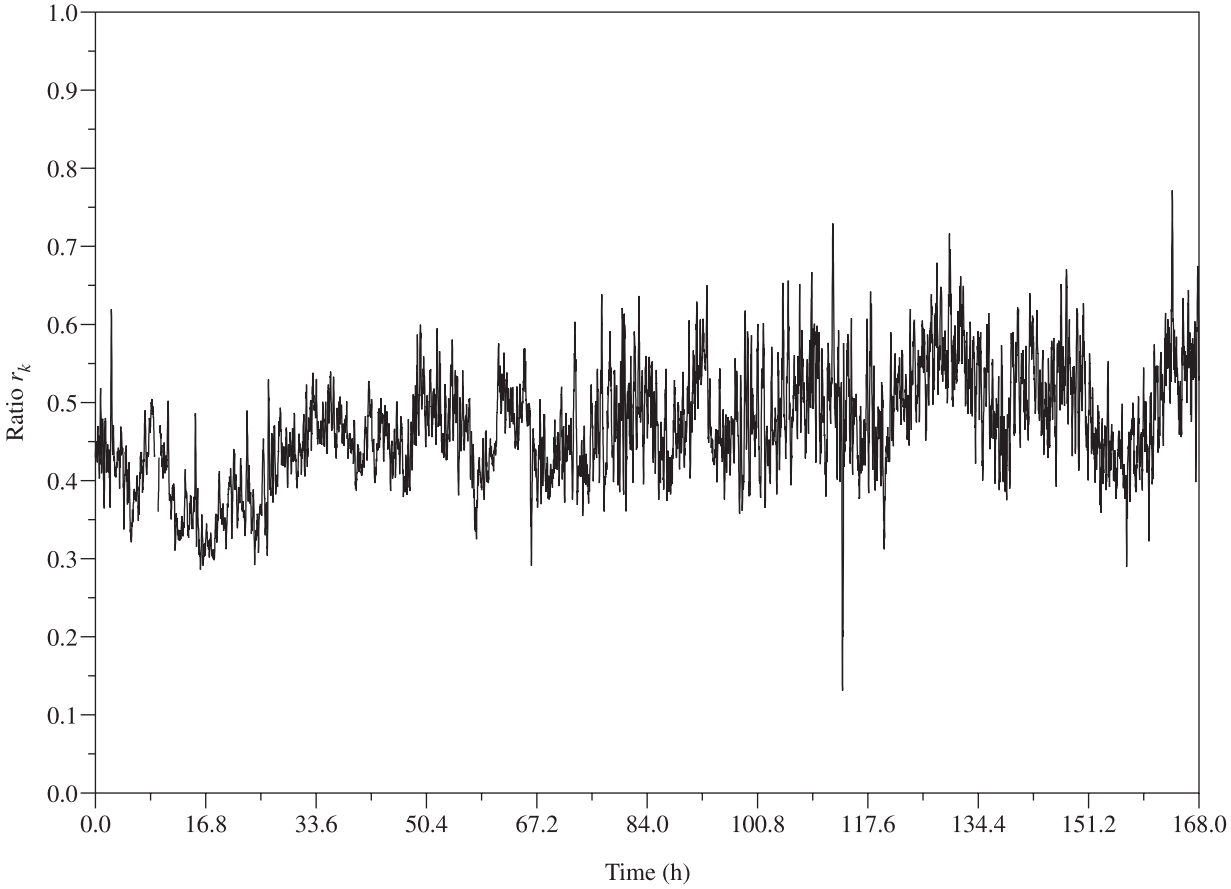

Observing in detail the time evolution of the inverse of the RSAM during the last few hours before the paroxysm, we can see that new decreasing trends appear, where the slope becomes steeper and steeper, pointing to a forecasted paroxysm that becomes closer and closer in the future. Figure 9 shows the same parameters as Fig. 8, but zooming in on the last 3 days before the paroxysm. Besides the previous fit (indicated by curve number 1 in Fig. 9*c*), two additional fits are calculated for the band-pass-filtered signal. Fit number 2 is calculated using data from 4 April 2003 at 2200 GMT to 5 April 2003 at 0000 GMT, and the forecasted time of occurrence of the paroxysm is 5 April 2003 at 1020 GMT. Fit number 3 is calculated using data from 5 April at 0500 GMT to 5 April at 0700 GMT, and the forecasted time of occurrence of the paroxysm is 5 April 2003 at 0913 GMT. Of course for this last fit, done over 2 h, we can only use six data points, with the windows being 20 min long.

Discussion

The detailed analysis of the seismic time series recorded at the summit station of University of Udine revealed a number of consistent variations in intensity, spectral, and dynamical parameters prior to the paroxysm of 5 April 2003. The intensity shows an increase, and the spectrum shows a general trend where energy consistently goes to lower frequencies, well summarized by the decrease in the average frequency. The dominant frequencies of the different seismic components show a convergence before the event. These variations all take place in the last 2.5 h before the event. Although these are not sufficient to define a real precursor, we claim that this is the minimum time scale at which the paroxysmal event built up.

Let us now try to interpret the trends we see in the dynamical parameters before the explosion. When we observe that before the paroxysmal event the system shows a decreasing number of FNNs for a given dimension, this means that the system dynamics become better and better explained in that dimension, i.e., it becomes simpler and simpler. The SVD then allows us to quantify how the dynamical system governing the volcano becomes simpler and simpler before the paroxysm. This behaviour can be explained using a phenomenon of auto-organization, where the dynamics show the buildup of consistent (and simpler) new structures in the phase space. This is consistent with a concentration of the energy in the lowest frequency ranges, as the scattered waves due, for example, to path effects lose importance with respect to the increasing source effects.

Although FNN and SVD give apparently similar information, it is important to monitor both, as they can show variations at slightly different times. In fact, even in a "stable" embedding dimension, an auto-organization can appear as a concentration of the trajectory in a limited part of the embedding space, highlighted by a discrepancy between FNN and SVD time

Fig. 8. Application of the material failure forecast method to Stromboli seismic data before the explosion of 5 April 2003. (*a*) As a reference, RSAM (in arbitrary units or A.U.) computed over 1 min time windows is plotted, computed over raw, unfiltered data. Vertical arrows indicate the most energetic explosions, the last one being the paroxysm of 5 April 2003. (*b*) Time evolution of the inverse of RSAM computed over raw unfiltered data using 20 min long windows. The least squares line is fitted to the data recorded from 3 April 2003 at 1230 GMT to 4 April 2003 at 1230 GMT. The intersection of this line with the horizontal axis gives the forecasted time of the paroxysm (6 April at 0100 GMT), and the circle indicates the actual occurrence of the paroxysm (5 April at 0712 GMT). (*c*) Time evolution of the inverse of the RSAM computed over band-pass-filtered data (FIR, center frequency 1.2 Hz, attenuation –80 dB at 0.5 and 2.0 Hz) using 20 min long windows. The least squares line is fitted to the data recorded from 3 April 2003 at 1230 GMT to 4 April 2003 at 1230 GMT. The intersection of this line with the horizontal axis gives the forecasted time of the paroxysm (5 April at 1500 GMT), and the circle indicates the actual occurrence of the paroxysm (5 April at 0712 GMT).

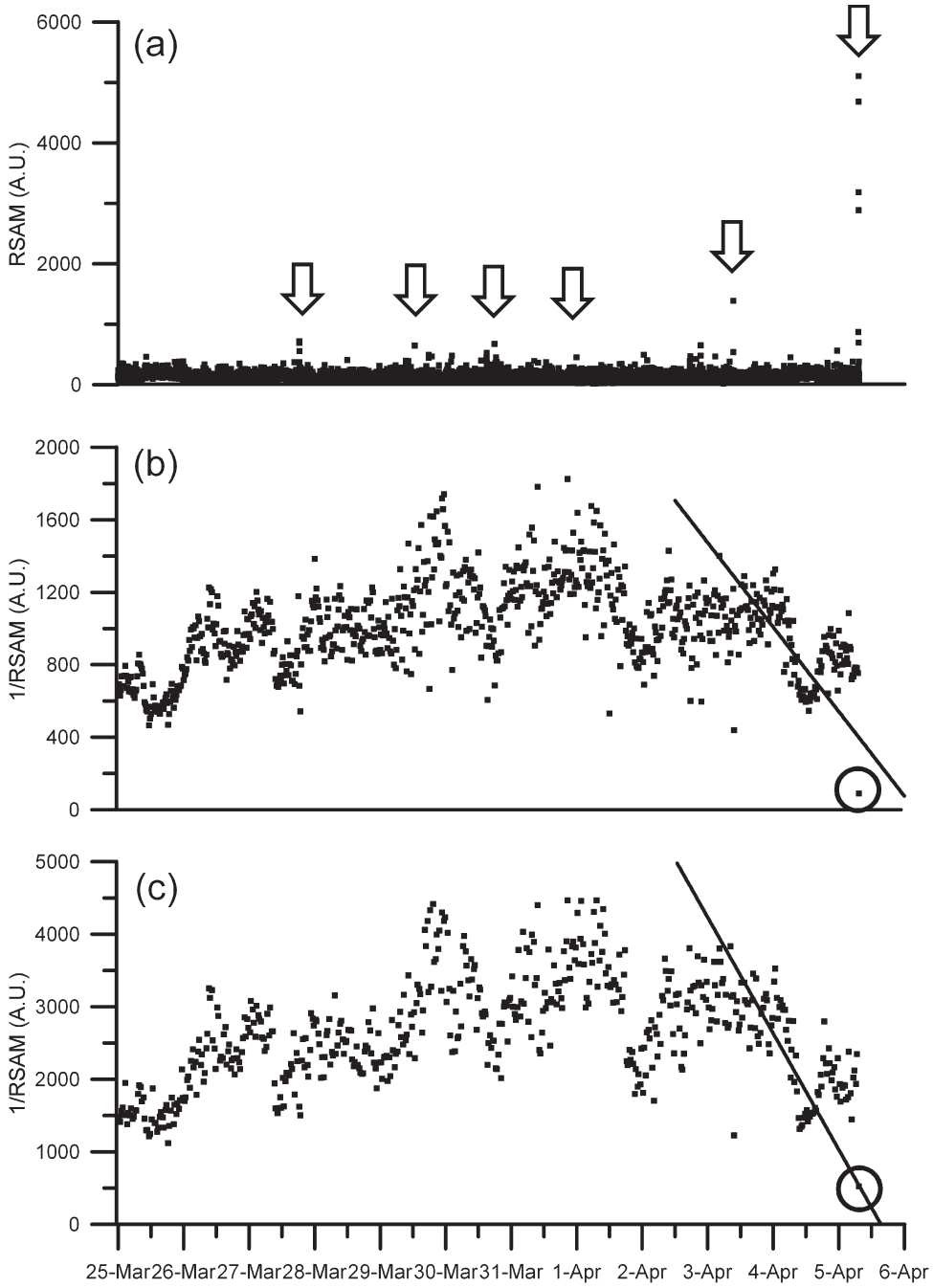

evolutions. This phenomenon was highlighted by Carniel and Di Cecca (1999), for example, for the case of the explosion of 1 June 1996 at Stromboli.

We have shown that the paroxysmal phase builds up over at least 2.5 h. However, is this the full time scale at which the phenomenon takes place? Moreover, can we try to fore-

Fig. 9. Application of the material failure forecast method to Stromboli seismic data before the explosion of 5 April 2003. This figure is similar to Fig. 8 but zooms in on the 3 days before the event. (*a*) As a reference, the RSAM computed over 1 min time windows is plotted, computed over raw, unfiltered data. Vertical arrows indicate the most energetic explosions, the last one being the paroxysm of 5 April 2003. (*b*) Time evolution of the inverse of the RSAM computed over raw unfiltered data using 20 min long windows. The least squares line is fitted to the data recorded from 3 April 2003 at 1230 GMT to 4 April 2003 at 1230 GMT. The intersection of this line with the horizontal axis gives the forecasted time of the paroxysm (6 April at 0100 GMT), and the circle indicates the actual occurrence of the paroxysm (5 April at 0712 GMT). (*c*) Time evolution of the inverse of the RSAM computed over band-pass-filtered data (FIR, center frequency 1.2 Hz, attenuation –80 dB at 0.5 and 2.0 Hz) using 20 min long windows. Line 1 is the least squares line fitted to the data recorded from 3 April 2003 at 1230 GMT to 4 April 2003 at 1230 GMT. The intersection of this line with the horizontal axis gives the forecasted time of the paroxysm (5 April at 1500 GMT). Line 2 is the least squares line fitted to the data recorded from 4 April 2003 at 2200 GMT to 5 April 2003 at 0000 GMT, leading to a forecast for the paroxysm of 5 April 2003 at 1020 GMT. Line 3 is based on data from 5 April at 0500 GMT to 5 April at 0700 GMT and forecasts the paroxysm for 5 April 2003 at 0913 GMT. The circle indicates the actual occurrence of the paroxysm (5 April at 0712 GMT).

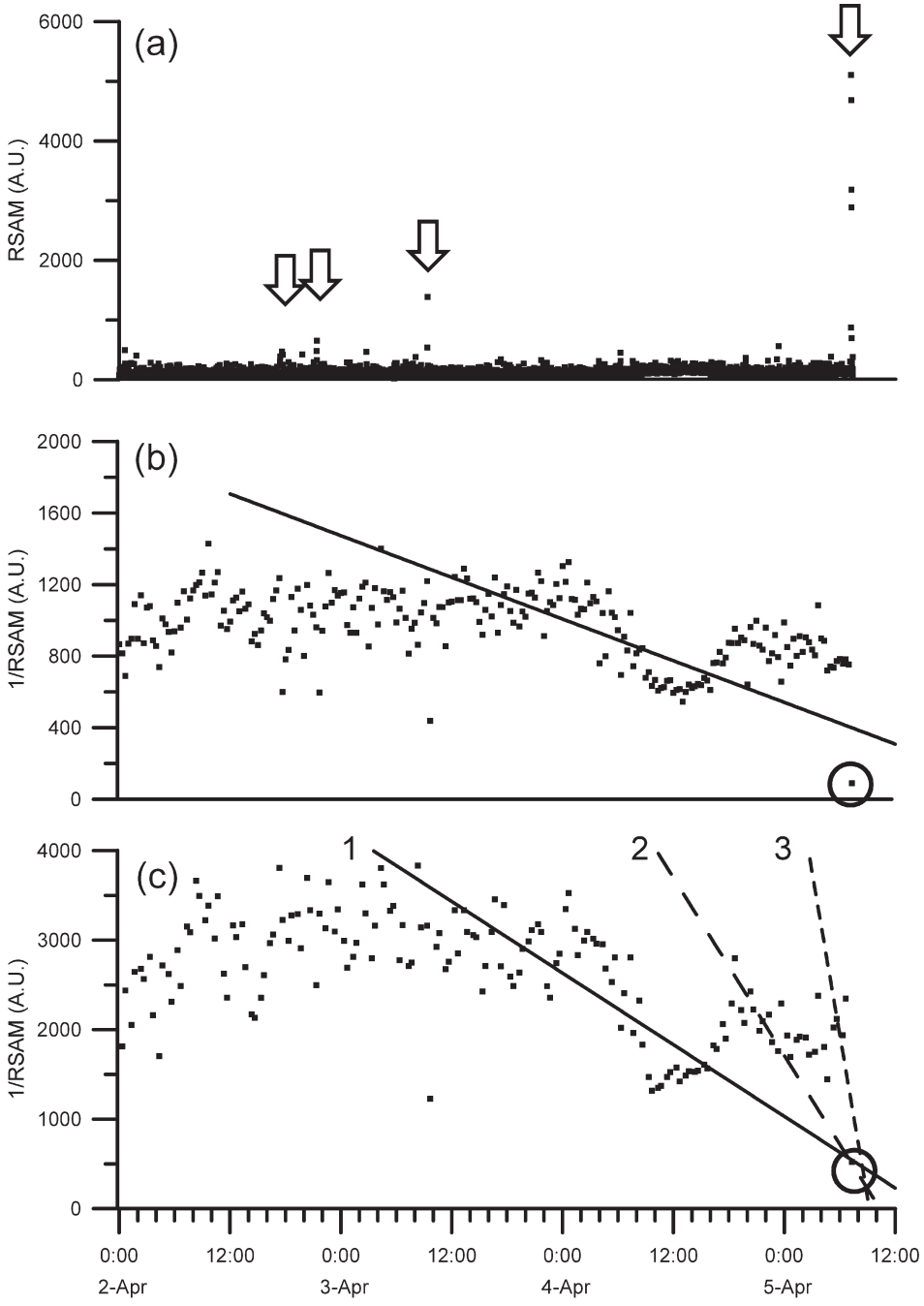

cast when the explosion is most likely to occur? We tried to answer this latter question through the application of the FFM. Once again, we found consistent decreasing trends that point to the paroxysmal event, highlighting another longer time scale, however, already 2 days before a forecast can be done that suggests a temporary increase of probability (TIP) of occurrence of a paroxysmal event for 5 April. This is generated using the consistent decreasing trend of 3–4 April that is also evident in the spectrogram with an increasing importance of the lower frequencies (cf. phase around hour 85 in Fig. 3), which is temporarily interrupted like an "aborted" evolution towards the paroxysmal phase forecasted for 5 April at 1500 GMT. This forecast is improved as we get closer and closer to the event. This is consistent with the increasing auto-organization of the system that culminates in the 2.5 h preceding the event in the dynamical phase already highlighted.

The fact that this final dynamical phase is somehow "anomalous" and we cannot simply say that the paroxysm happened in the middle of a consistent but "normal" dynamical phase is confirmed by the time evolution of the SVD ratios, which show values never before observed during the previous 2 weeks. This also helps to discern this decreasing trend of the inverse of RSAM from other, short-lived decreasing phases, leading to explosions only slightly more energetic than the normal strombolian activity. None of the single parameter variations is, therefore, significant if used alone but becomes significant in the light of the evolution of the others.

Moreover, it is important to note that a TIP does not imply that a paroxysm will necessarily occur. This may require a final trigger to be accelerated to the paroxysm, like an earthquake in the case of the Mount St. Helens eruption. Moreover, as the material failure is a highly nonlinear phenomenon, we can see the evidence of its acceleration only shortly before the paroxysm, although the general buildup of a "suitable" state of the volcano may take place slowly weeks in advance (Sparks 2003).

Conclusions

The explosion of 5 April 2003 was a paroxysm comparable in size to that observed in 1930. It is most probable that no casualties were caused by the explosion because of the access limitations issued by the Italian Civil Defence after the 30 December 2002 landslide and tsunami. Moreover, the time of the explosion helped to prevent casualties, including among the scientists. Forecasting a similar event would therefore be of the utmost importance.

Although classical routine analysis of a complete geophysical and geochemical data set available to the Italian Civil Defence did not show any visible precursor, performing a thorough analysis of a single seismic data series provided a series of useful hints.

The analysis of the time evolution of a series of rather classical linear parameters (intensity, spectrogram, and main and average frequencies) suggested the presence of a consistent dynamical phase, lasting about 2.5 h before the explosion. The application of more sophisticated dynamical tools (autocorrelation first zero and redundancy first minimum time delay estimators and FNN percentages) provides further evidence for the hypothesis of a consistent dynamical behaviour during the last few hours. In particular, the FNN percentage in dimension 8 revealed itself as a first candidate for the possible role of precursor. Similar values for this parameter were also observed, however, during the previous 2 weeks.

Subdivision of the dynamics into lower and higher dimensions through the SVD went even farther, that is, up to highlighting the relative importance of the lowest dimensions never as high as during the phase preceding the paroxysm. This suggests a phenomenon of auto-organization of the system.

The application of a completely different methodology, i.e., the material failure forecast method, applied to the data recorded during the days before the event revealed a consistent trend that suggests a preparation of the paroxysm farther into the past, an evolution that was possibly temporarily "aborted" or simply "paused" the day before, before finally accelerating during the consistent dynamical phase of the last few hours before the event. Applying a fit to different phases of this accelerating dynamics provides increasingly accurate forecasts.

All these observations strongly suggest that the continuous signals have a high information content that should be better exploited than has been done to date. The time evolution of the continuous signals (of which the volcanic tremor is just one example) can provide a number of parameters to a volcano observatory (and (or) Civil Defence organization) that have the same (or more) forecast potential as that of the statistics usually computed based on discrete events (e.g., number of events in a given classification).

Of course, none of these parameters alone can or should be considered a precursor in itself. Inclusion of all of the parameters, however, together with those computed from all the other observables available to Civil Defence and properly weighted by a probabilistic approach such as the Bayesian belief network (Aspinall et al. 2003, in preparation) could lead to a usable estimate of the so-called TIP of occurrence of a paroxysm.

Acknowledgments

The dynamical methodology and software development by R. Carniel and M. Di Cecca is supported by the European Community MULTIMO project, European Union (EU) contract number EVG1-CT-2000-00021. Ramon Ortiz is supported by the European Community e-Ruption project, EU contract number EVR1-CT-2000-40021. The SCILAB package (see http://www.scilab.org) was used to integrate the different analysis routines. Italian Civil Defence provided logistic support when access to the summit area was forbidden. The seismic station was originally installed under a research grant from the Italian Gruppo Nazionale di Vulcanologia. The authors gratefully acknowledge the collaboration of J. Alean, S. Ballarò, F. Barazza, S. Calvari, C. Cardaci, M. Fulle, A. Garcia, A. Llinares, V. Perin, M. Ripepe, and M. Tarraga in the various stages of data acquisition, logistical help, data analysis, interpretation, and manuscript reviewing. The comments of the reviewers Richard Luckett and Georgia Pe-Piper and the Associate Editor John D. Greenough greatly improved the quality of this manuscript.

References

Alean, J., Carniel, R., and Fulle, M. 2005. Stromboli online — volcanoes of the world: information on Stromboli, Etna and other volcanoes. Available from < http://stromboli.net >.

Aspinall, W.P., Woo, G., Voight, B., and Baxter, P.J. 2003. Evidence-based volcanology: application to eruption crises. Journal of Volcanology and Geothermal Research, **128**: 273–285.

Aspinall, W.P., Carniel, R., Jaquet, O., and Woo, G., and Hincks, T., In 2006. Using Hidden Multi-state Markov models with multi-parameter volcanic data to provide empirical evidence for alert level decision-support. Journal of Volcanology and Geothermal Research. In press. Available online: DOI 10.1016/j.jvolgeores.2005.08.010.

Barberi, F., Rosi, M., and Sodi, A. 1993. Volcanic hazard assessment at Stromboli based on review of historical data. Acta Vulcanologica, **3**: 173–187.

Barberi, F., Carapezza, M.L., Alean, J., and Carniel, R. 2001. Stromboli report. Smithsonian Institution Global Volcanism Network Bulletin, **26**(10): 2–3.

Beinat, A., Carniel, R., and Iacop, F. 1994. Seismic station of Stromboli: 3-component data acquisition system. Acta Vulcanologica, **5**: 221–222.

Bonaccorso, A., Calvari, S., Garfì, G., Lodato, L., and Patanè, D. 2003. Dynamics of the December 2002 flank failure and tsunami at Stromboli volcano inferred by volcanological and geophysical observations. Geophysical Research Letters, **30**(18): 1941–1944.

Broomhead, D.S., and King, G.P. 1986. Extracting qualitative dynamics from experimental data. Physica D, **20**: 217–236.

Calvari, S. 2003*a*. Stromboli report. Smithsonian Institution Global Volcanism Network Bulletin, **28**(4): 8–9.

Calvari, S. 2003*b*. Stromboli report. Smithsonian Institution Global Volcanism Network Bulletin, **28**(8): 5.

Calvari, S., and Stromboli On Line. 2002. Stromboli report. Smithsonian Institution Global Volcanism Network Bulletin, **27**(12): 20.

Carniel, R., and Di Cecca, M. 1999. Dynamical tools for the analysis of long term evolution of volcanic tremor at Stromboli. Annali di Geofisica, **42**(3): 483–495.

Carniel, R., and Iacop, F. 1996*a*. On the persistency of crater assignment criteria for Stromboli explosion-quakes. Annali di Geofisica, **39**(2): 347–359.

Carniel, R., and Iacop, F. 1996*b*. Spectral precursors of paroxysmal phases of Stromboli. Annali di Geofisica, **39**(2): 327–345.

Carniel, R., Di Cecca, M., and Rouland, D. 2003. Ambrym, Vanuatu (July–August 2000): spectral and dynamical transitions on the hours-to-days time scale. Journal of Volcanology and Geothermal Research, **128**(1–3): 1–13.

Chouet, B.A., and Shaw, H.R. 1991. Fractal properties of tremor and gas-piston events at Kilauea Volcano, Hawaii. Journal of Geophysical Research, **96**: 10 177 – 10 189.

Cornelius, R.R., and Voight, B. 1995. Graphical and PC-software analysis of volcano eruption precursors according to the Materials Failure Forecasting Method (FFM). Journal of Volcanology and Geothermal Research, **64**: 295–320.

De la Cruz-Reyna, S., and Reyes-Dávila, G. 2001. A model to describe precursory material-failure phenomena: application to short-term forecasting at Colima volcano, Mexico. Bulletin of Volcanology, **63**: 297–308.

Endo, T.E., and Murray, T. 1991. Real-time seismic amplitude measurement (RSAM): a volcano monitoring and prediction tool. Bulletin of Volcanology, **53**: 533–545.

Falsaperla, S., and Spampinato, S. 1999. Tectonic seismicity at Stromboli volcano (Italy) from historical data and seismic records. Earth and Planetary Science Letters, **173**(4): 425–437.

Falsaperla, S., Langer, H., and Spampinato, S. 1998. Statistical analyses of volcanic tremor on Stromboli volcano (Italy). Bulletin of Volcanology, **60**: 75–88.

Falsaperla, S., Alparone, S., and Spampinato, S. 2003. Seismic features of the June 1999 tectonic swarm in the Stromboli volcano region, Italy. Journal of Volcanology and Geothermal Research, **125**(1–2): 121–136.

Francalanci, L., Tommasini, S., and Conticelli, S. 2004. The volcanic activity of Stromboli in the 1906–1998 AD period: mineralogical, geochemical and isotope data relevant to the understanding of the plumbing system. Journal of Volcanology and Geothermal Research, **131**: 179–211.

Harris, A.J., Carniel, R., and Jones, J. 2005. Identification of variable convective regimes at Erta Ale Lava Lake. Journal of Volcanology and Geothermal Research, **142**(3–4): 207–223.

Jaquet, O., and Carniel, R. 2001. Stochastic modelling at Stromboli: a volcano with remarkable memory. Journal of Volcanology and Geothermal Research, **105**: 249–262.

Jaquet, O., and Carniel, R. 2003. Multivariate stochastic modelling: towards forecasts of paroxysmal phases at Stromboli. Journal of Volcanology and Geothermal Research, **128**(1–3): 261–271.

Jaquet, O., Carniel, R., Sparks, S., Thompson, G., Namar, R., and Di Cecca, M. 2006. DEVIN: a forecasting approach using stochastic methods applied to the Soufrière Hills volcano. Journal of Volcanology and Geothermal Research. In press. Available online: DOI 10.1016/j.jvolgeores.2005.08.013.

Jaupart, C., and Vergniolle, S. 1989. The generation and collapse of a foam layer at the roof of a basaltic magma chamber. Journal of Fluid Mechanics, **203**: 347–380.

Jones, J., Carniel, R., Harris, A.J.L., and Malone, S. 2006. Seismic characteristics of variable convection at Erta Ale lava lake, Ethiopia. Journal of Volcanology and Geothermal Research. In press. Available online: DOI 10.1016/j.jvolgeores.2005.08.004.

Kazahaya, K., Shinohara, H., and Saito, G. 1994. Excessive degassing of Izu-Oshima volcano: magma convection in a conduit. Bulletin of Volcanology, **56**: 207–216.

Kennel, M.B., Brown, R., and Abarbanel, H.D.I. 1992. Determining embedding dimension for phase-space reconstruction using a geometrical construction. Physical Review A, **45**(6): 3403–3411.

Konstantinou, K.I., and Schlindwein, V. 2002. Nature, wavefield properties and source mechanisms of volcanic tremor: a review. Journal of Volcanology and Geothermal Research, **119**: 161–187.

Martinelli, B. 1997. Volcanic tremor and short-term prediction of eruptions. Journal of Volcanology and Geothermal Research, **77**: 305–311.

Ortiz, R., García, A., and Astiz, M. 2001. Instrumentación en Volcanología. Servicio de Publicaciones del Cabildo Insular de Lanzarote, Madrid, Spain, 345 p. [ISBN 84-87021-84-0].

Ortiz, R., Moreno, H., García, A., Fuentealba, G., Astiz, M., Peña, P., Sánchez, N., and Tárraga, M. 2003. Villarrica Volcano (Chile): characteristics of the volcanic tremor and forecasting of small explosions by means of materials failure method. Journal of Volcanology and Geothermal Research, **128**(1–3): 247–259.

Packard, N.H., Crutchfield, J.P., Farmer, J.D., and Shaw, R.S. 1980. Geometry from a time series. Physical Review Letters, **45**(9): 712–716.

Parfitt, E.A., and Wilson, L. 1995. Explosive volcanic eruptions — IX: the transition between Hawaiian-style lava fountaining and Strombolian explosive activity. Geophysical Journal International, **121**: 226–232.

Ripepe, M., and Gordeev, E. 1999. Gas bubble dynamics model for

shallow volcanic tremor at Stromboli. Journal of Geophysical Research, **104**(B5): 10 639 – 10 654.

Ripepe M., Ciliberto, S., and Della Schiava, M. 2001. Time constraint for modelling source dynamics of volcanic explosions at Stromboli. Journal of Geophysical Research, **106**(B5): 8713–8727.

Ripepe, M., Harris, A.J.L., and Carniel, R. 2002. Thermal, seismic and infrasonic evidences of variable degassing rates at Stromboli volcano. Journal of Volcanology and Geothermal Research, **118**: 285–297.

Rosi, M., Bertagnini, A., and Landi, P. 2000. Onset of the persistent activity at Stromboli Volcano (Italy). Bulletin of Volcanology, **62**: 294–300.

Sparks, R.S.J. 2003. Forecasting volcanic eruptions. Earth and Planetary Science Letters, **210**: 1–15.

Stevenson, D.S., and Blake, S. 1998. Modelling the dynamics and thermodynamics of volcanic degassing. Bulletin of Volcanology, **60**: 307–317.

Thomas, N., Tait, S., and Koyaguchi, T. 1993. Mixing of stratified liquids by the motion of gas bubble: application to magma mixing. Earth and Planetary Science Letters, **115**: 161–175.

Tibaldi, S. 2004. Major changes in volcano behaviour after a sector collapse: insights from Stromboli, Italy. Terra Nova, **16**(1): 2–8.

Tokarev, P.I. 1963. On a possibility of forecasting of Bezimianny volcano eruptions according to seismic data. Bulletin of Volcanology, **26**: 379–386.

Urquizú, M., and Correig, A. 1999. On the spectral peaks of volcanic tremor at Stromboli. Physics of the Earth and Planetary Interiors, **110**: 247–261.

Voight, B. 1988. A method for prediction of volcanic eruptions. Nature (London), **332**(10): 125–130.

Voight, B. 1989. A relation to describe rate-dependent material failure. Science (Washington, DC), **243**: 200–203.

Voight, B., and Cornelius, R.R. 1991. Prospects for eruption prediction in near real-time. Nature (London), **350**: 695–698.

Wilson, L., and Head, J.W. 1981. Ascent and eruption of basaltic magma on the Earth and Moon. Journal of Geophysical Research, **86**: 2971–3001.